

Probing attosecond pulses by XUV stimulated dynamics

J. Marcus Dahlström

PhD: Lund [LTH] -> Post-doc: Stockholm [SU] -> Guest res.: Hamburg [CFEL/MPGPKS]
-----*
2015-05-27 Nordita, Stockholm, Sweden.



MAX-PLANCK-GESellschaft

AlbaNova

MPG-PKS

J. Marcus Dahlström

Probing attosecond pulses by XUV stimulated dynamics

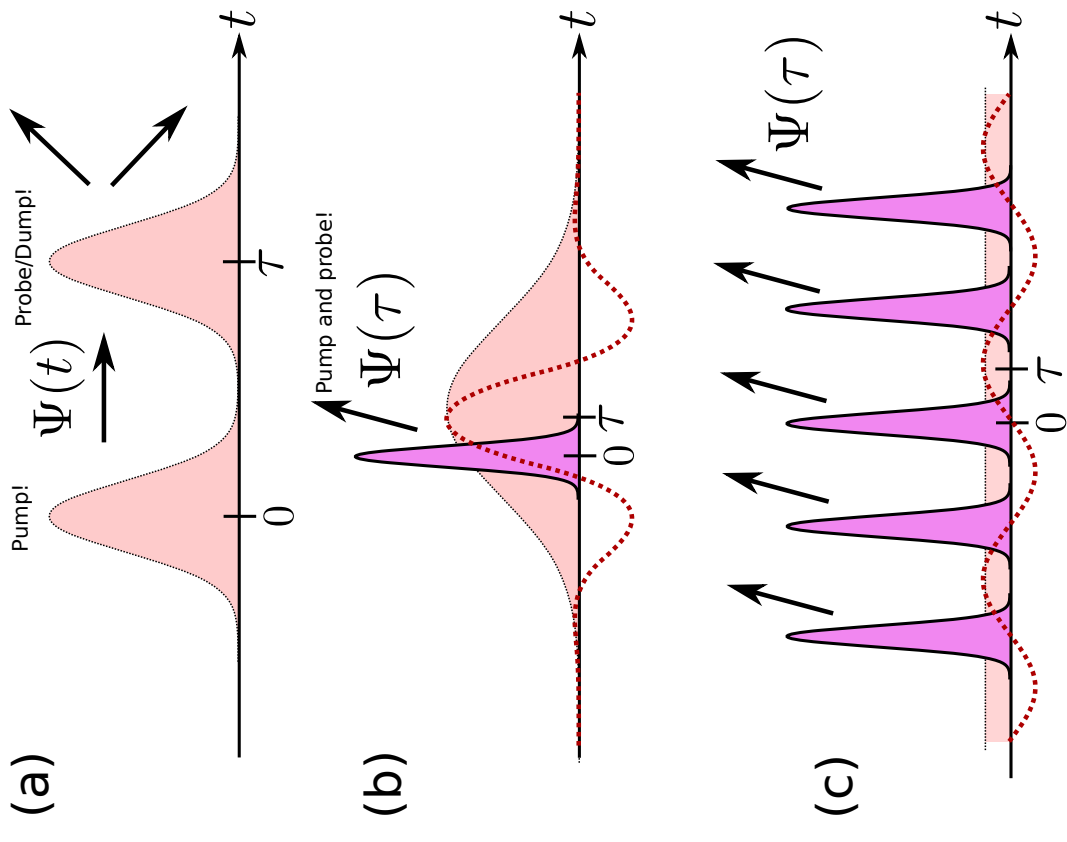
Outline of talk:

- Introduction to “attophysics”
- Details on computational method (SU: MBPT)
- New proposal:
Attosecond interferometry based on stimulated hole dynamics

Introduction to “attophysics”

Overview of pump and probe setups

Traditional pump and probe
with *femto-pulses* control of
Born-Oppenheimer dynamics:



$$(1 \text{ as} = 10^{-3} \text{ fs} = 10^{-18} \text{ s})$$

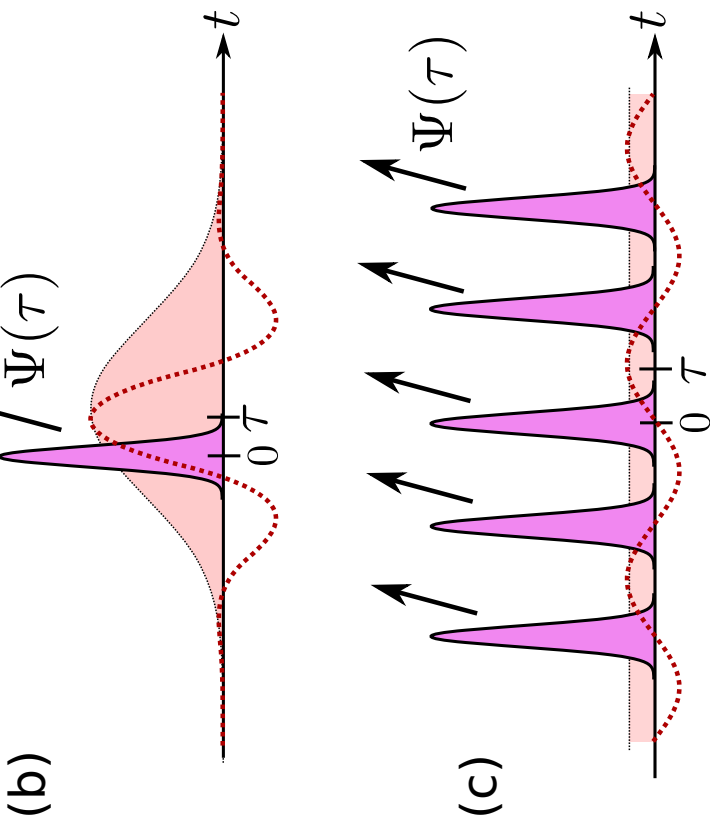
Introduction to “attophysics”

Overview of pump and probe setups

Traditional pump and probe
with *femto-pulses* control of
Born-Oppenheimer dynamics:
- Tannor-Rice: (t -domain)
- Brumer-Shapiro: (ω -dom.)

(a)

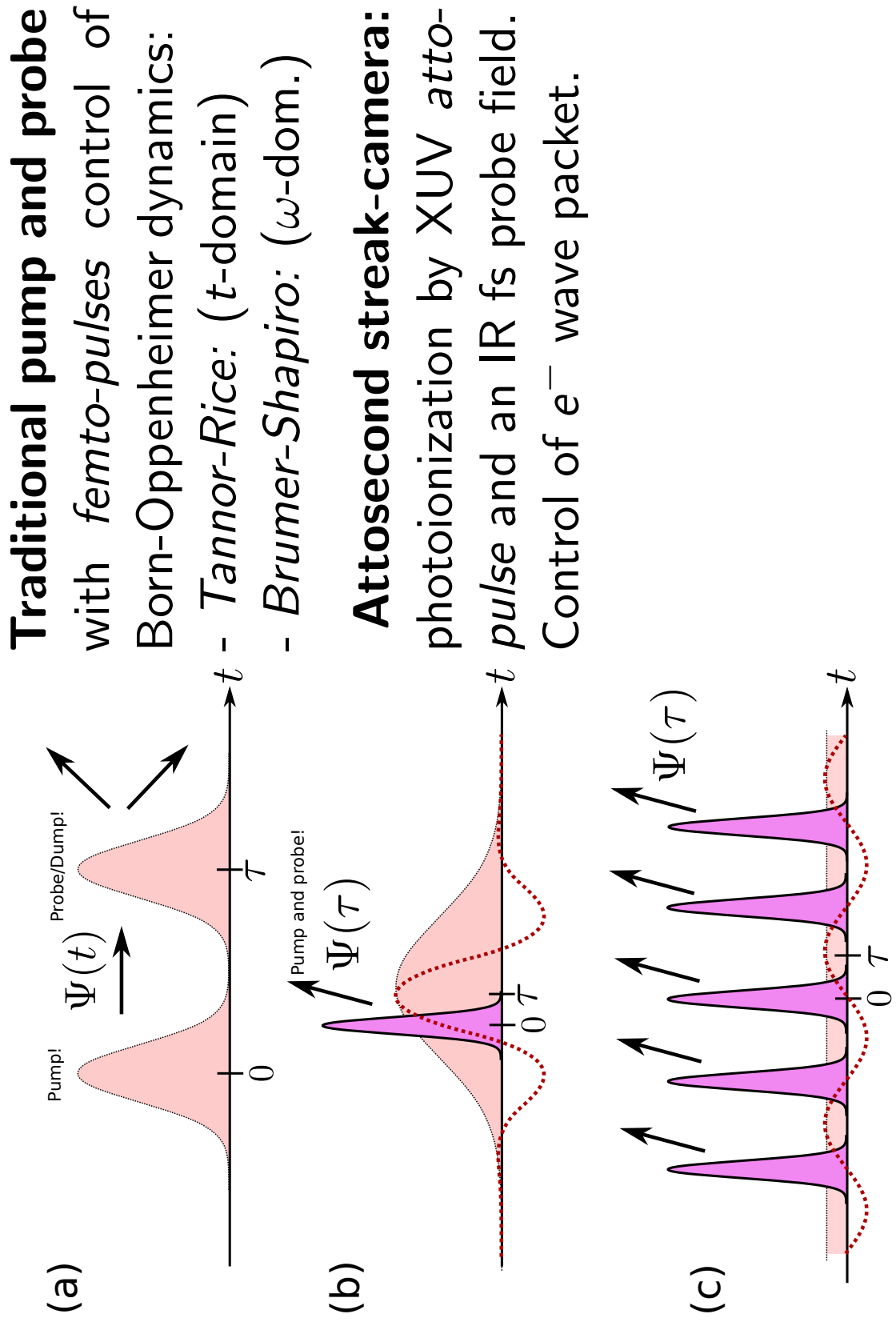
(b)



$$(1 \text{ as} = 10^{-3} \text{ fs} = 10^{-18} \text{ s})$$

Introduction to “attophysics”

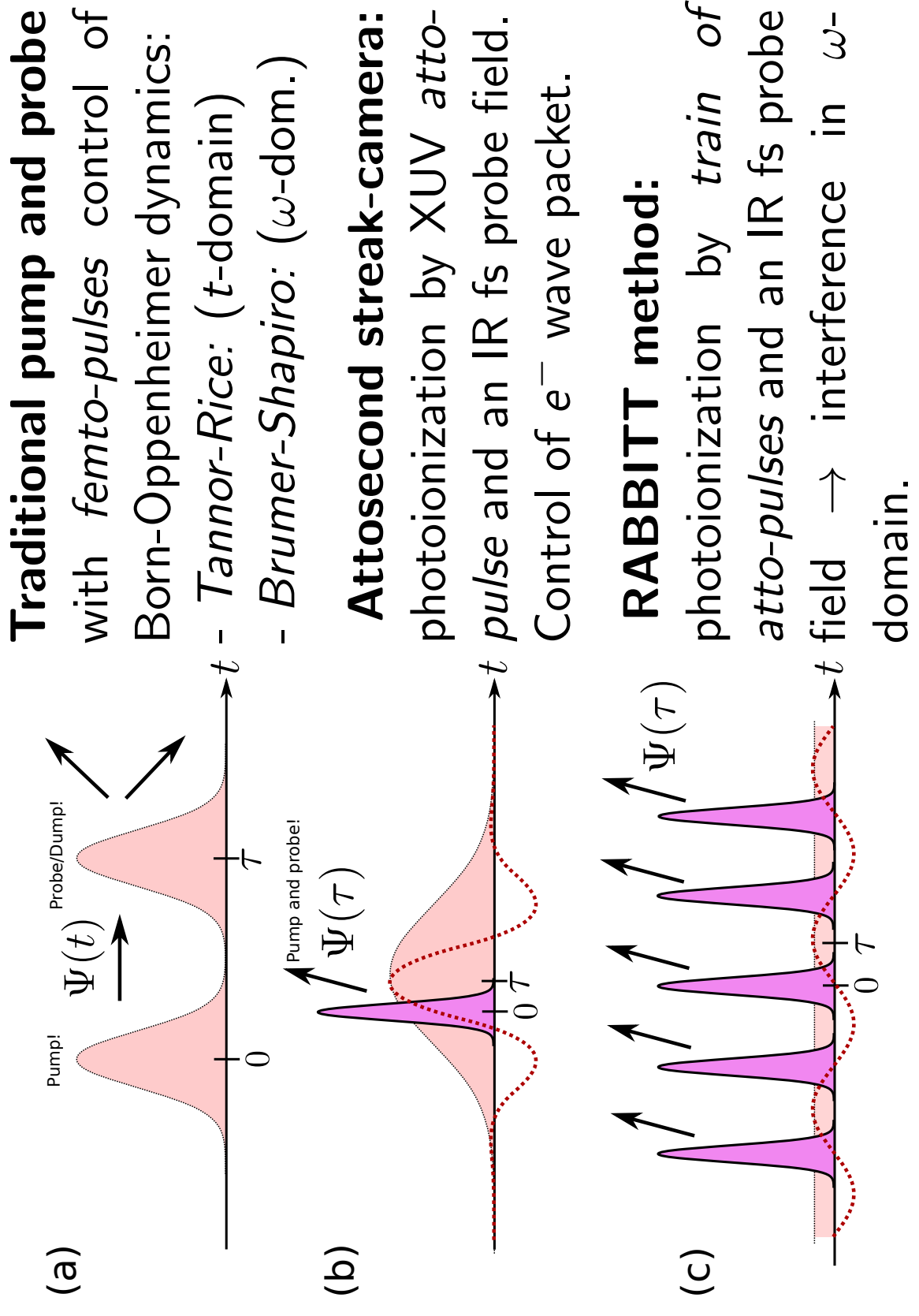
Overview of pump and probe setups



$$(1 \text{ as} = 10^{-3} \text{ fs} = 10^{-18} \text{ s})$$

Introduction to “attophysics”

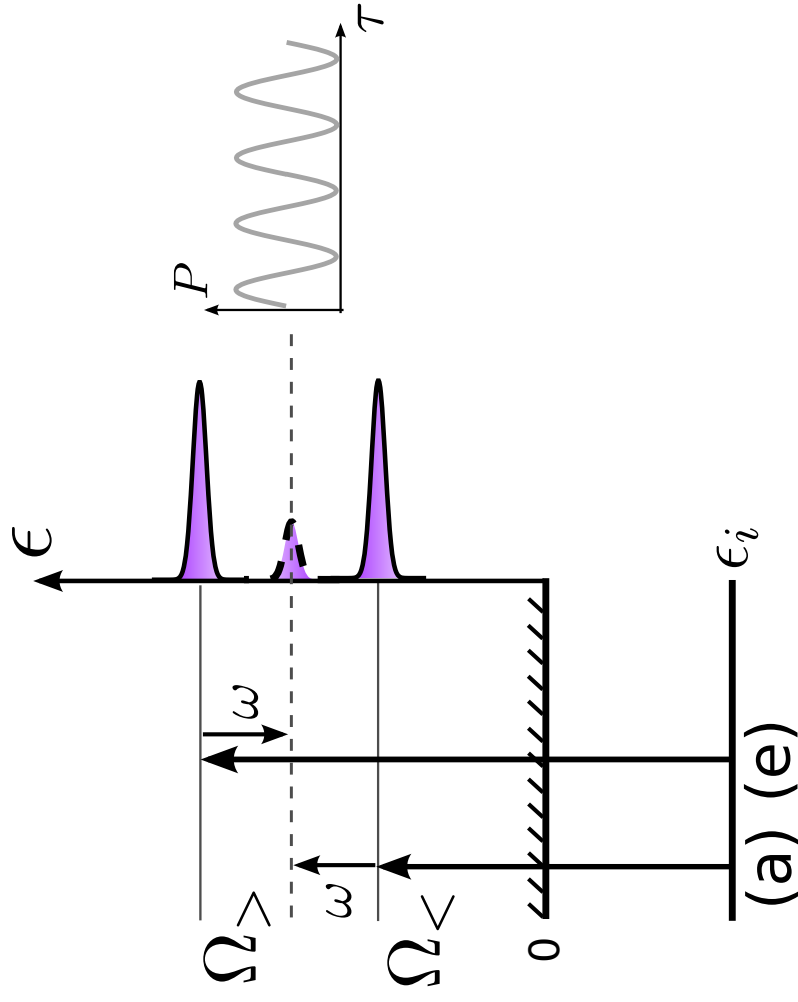
Overview of pump and probe setups



Introduction to “attophysics”

Reconstruction of Attosecond Beating by Interference of Two-photon Transitions:

Attosecond pulse train \rightarrow odd XUV harmonics: $(2q + 1)\omega$.

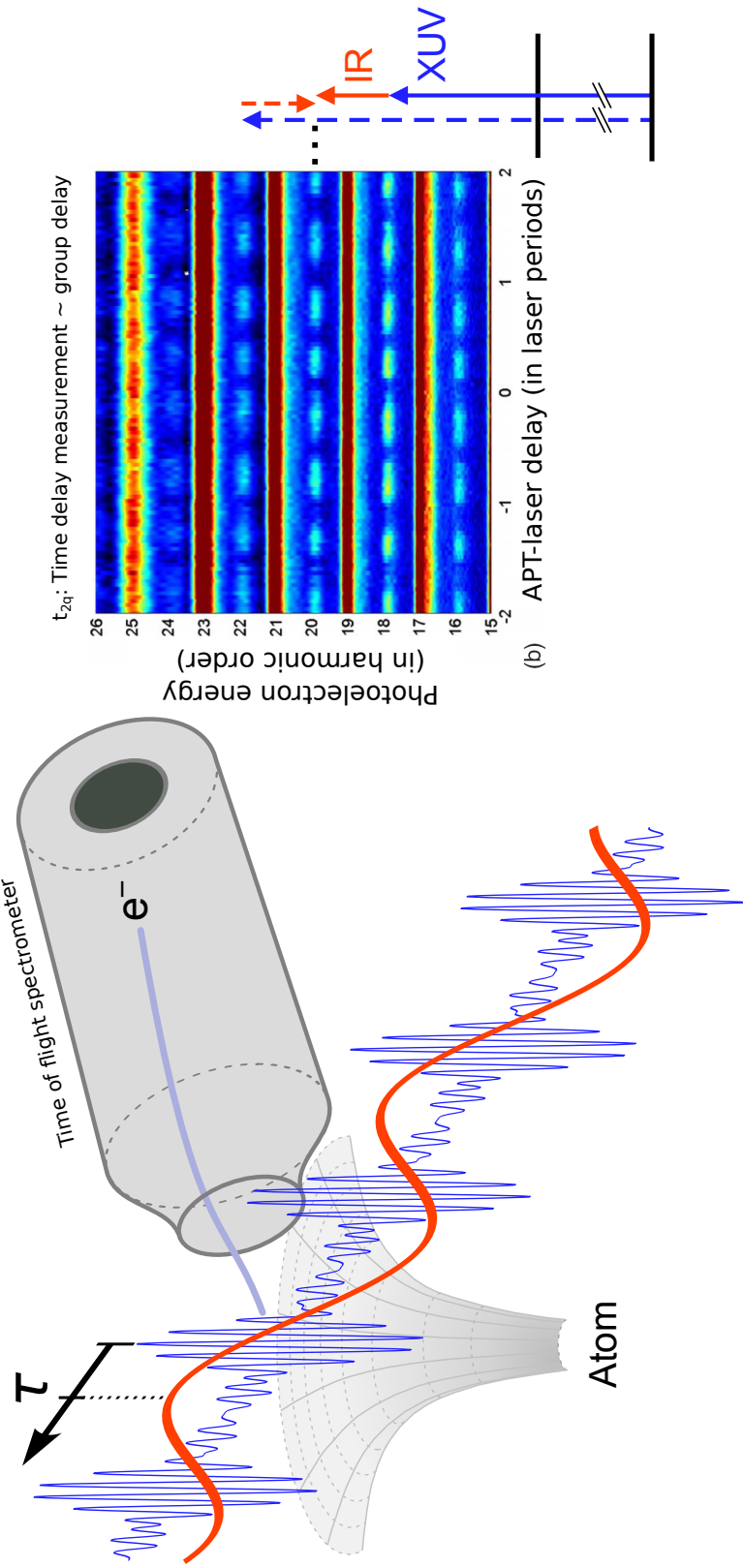


Experiment: Paul et al. *Science* (2001) 292 1689

Theory: Muller (2002) *Appl. Phys. B* 74 s17-21

Atomic delay in *single* ionization

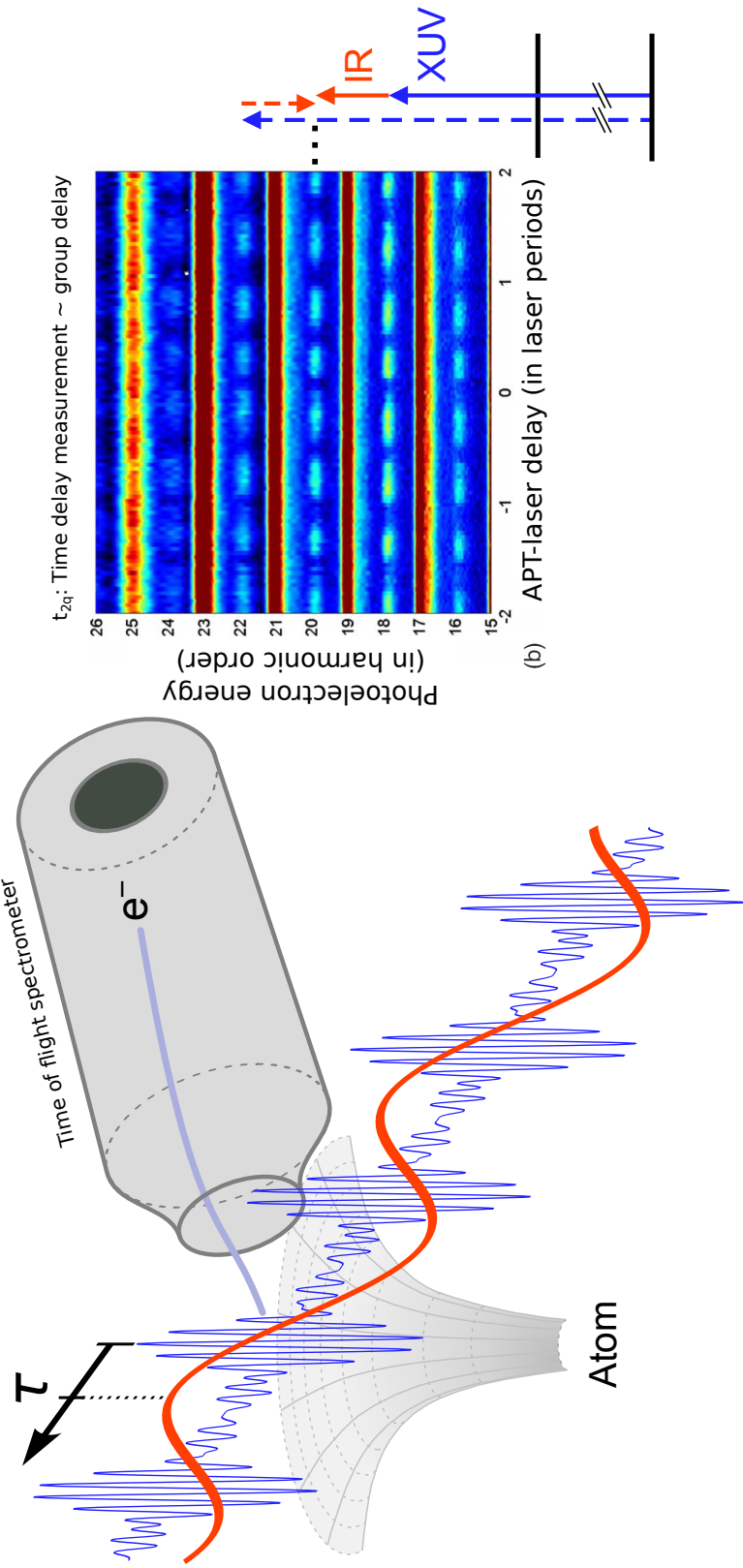
Sketch of the RABBITT setup



- *Time-of-flight* tube determines the *energy* of the electron.

Atomic delay in *single* ionization

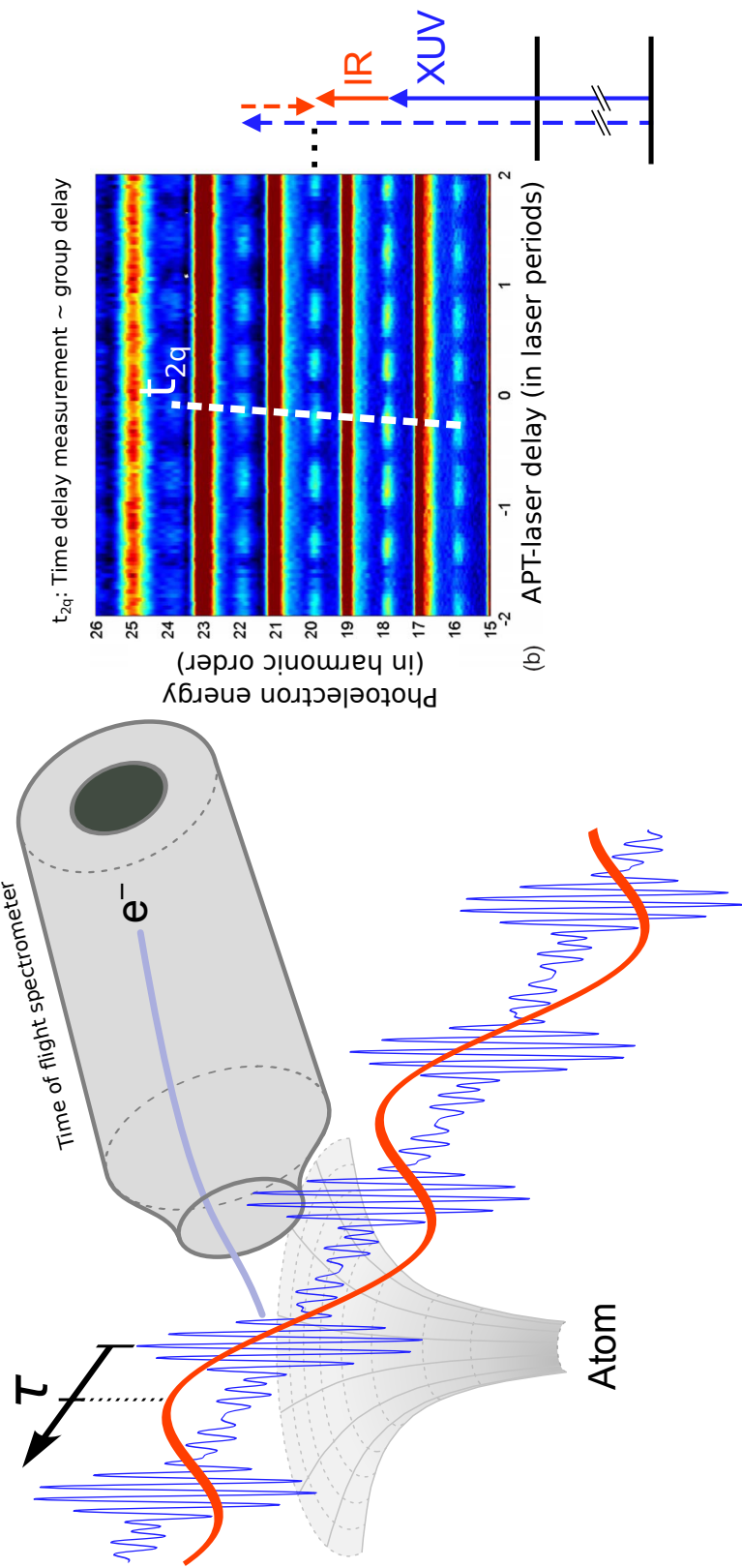
Sketch of the RABBITT setup



- *Time-of-flight* tube determines the *energy* of the electron.
- Information about the *delay* of the wave packet is found in modulations of the *sidebands* over pump-probe delay.

Atomic delay in *single* ionization

Sketch of the RABBITT setup



- *Time-of-flight* tube determines the *energy* of the electron.
- Information about the *delay* of the wave packet is found in modulations of the *sidebands* over pump-probe delay.

Inter-species photoionization delay experiment

(in attoseconds, $1 \text{ as} = 10^{-18} \text{ s}$)

Sideband	20	22	24
$\tau(\text{Ar}) - \tau(\text{Ne})$	68 ± 15	70 ± 12	52 ± 25
Theory	60	51	40
$\tau(\text{Ar}) - \tau(\text{He})$	82 ± 15	83 ± 22	71 ± 21
Theory	72	59	45
$\tau(\text{Ne}) - \tau(\text{He})$	23 ± 4	12 ± 4	10 ± 8
Theory	12	8	4

The delay is relative to the same sideband order.

- Ar has a larger delay than both Ne and He.
- Theory shows slightly smaller delays.

[Guénnot et al 2014 J. Phys. B: At. Mol. Opt. Phys. 47 245602]:

Inter-species photoionization delay experiment

(in attoseconds, $1 \text{ as} = 10^{-18} \text{ s}$)

Sideband	20	22	24
$\tau(\text{Ar}) - \tau(\text{Ne})$	68 ± 15	70 ± 12	52 ± 25
Theory	60	51	40
$\tau(\text{Ar}) - \tau(\text{He})$	82 ± 15	83 ± 22	71 ± 21
Theory	72	59	45
$\tau(\text{Ne}) - \tau(\text{He})$	23 ± 4	12 ± 4	10 ± 8
Theory	12	8	4

The delay is relative to the same sideband order.

- Ar has a larger delay than both Ne and He.
- Theory shows slightly smaller delays.

The RABBITT method is *not perfect for attosecond metrology because we measure different delays for different target atoms.*

[Guénnot et al 2014 J. Phys. B: At. Mol. Opt. Phys. 47 245602]:

Method

Diagrammatic Many-Body Perturbation Theory with Photons

Independent electron Hamiltonian:

$$h_\ell(r) = -\frac{1}{2} \frac{d^2}{d^2 r} + \frac{\ell(\ell+1)}{2r^2} - \frac{Z}{r} + u_{HF}(r) + u_Q(r)$$

Restricted Hartree-Fock (sum orbitals b with occupancy q_b):

$$u_{HF}(r) = \sum_b q_b [J_b(r) - \frac{1}{2} K_b(r)],$$

Method

Diagrammatic Many-Body Perturbation Theory with Photons

Independent electron Hamiltonian:

$$h_\ell(r) = -\frac{1}{2} \frac{d^2}{d^2 r} + \frac{\ell(\ell+1)}{2r^2} - \frac{Z}{r} + u_{HF}(r) + u_Q(r)$$

Restricted Hartree-Fock (sum orbitals b with occupancy q_b):

$$\begin{aligned} u_{HF}(r) &= \sum_b q_b [J_b(r) - \frac{1}{2} K_b(r)], \\ J_b(r) P_a(r) &= \sum_k c(abk) \frac{1}{r} Y_k(bb, r) P_a(r), \\ K_b(r) P_a(r) &= -2 \sum_k d(abk) \frac{1}{r} Y_k(ab, r) P_b(r), \\ Y_k(ab, r) &= r \int_0^\infty dr' \frac{r'_<^k}{r'_>^{k+1}} P_a(r') P_b(r') \end{aligned}$$

Lindgren and Morisson *Atomic Many-Body Theory*, Springer (1982)

Method

Projected potential $u_Q(r)$ alters excited electron orbitals

Excited electrons should see a long range $-1/r$ potential:

$$\begin{aligned} u_Q &= -\hat{Q} \frac{1}{r} J_0(a a, r) \hat{Q}, \\ \hat{P} &= \sum_a^{\text{occ}} | P_a \rangle \langle P_a | \\ \hat{Q} &= \sum_p^{\text{exc}} | P_p \rangle \langle P_p |, \end{aligned}$$

The **projected potential ensures Rydberg series** and Coulombic asymptotic wavefunctions for excited states.

See also: *Dahlström and Lindroth J. Phys. B (2014) 47 124012*

Method

Projected potential $u_Q(r)$ alters excited electron orbitals

Excited electrons should see a long range $-1/r$ potential:

$$\begin{aligned} u_Q &= -\hat{Q} \frac{1}{r} J_0(a a, r) \hat{Q}, \\ \hat{P} &= \sum_a^{\text{occ}} | P_a \rangle \langle P_a | \\ \hat{Q} &= \sum_p^{\text{exc}} | P_p \rangle \langle P_p |, \end{aligned}$$

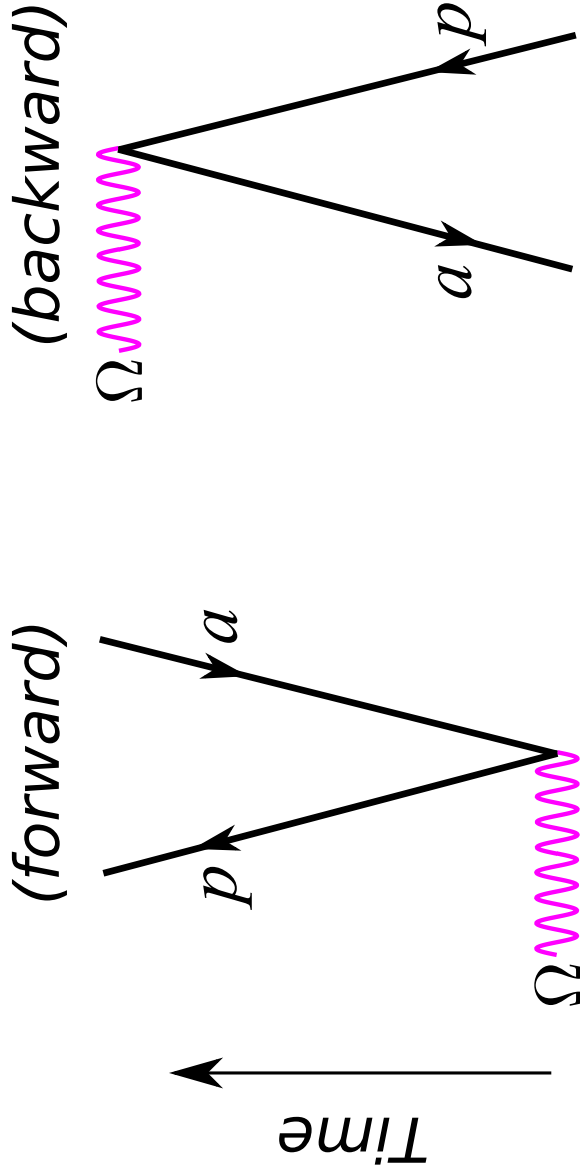
The **projected potential ensures Rydberg series** and Coulombic asymptotic wavefunctions for excited states.

Fermi vacuum (second quantization): $1 = \hat{P} + \hat{Q}$.
Holes ($\downarrow \in \hat{P}$ occupied) and electrons ($\uparrow \in \hat{Q}$ excited).

See also: *Dahlström and Lindroth J. Phys. B (2014) 47 124012*

Diagrammatic perturbation theory

Setup of uncorrelated perturbed wavefunction



$$\rho_{fwd}(a) = \sum_p \frac{\langle p | \dots | p \rangle \langle p | d_\Omega | a \rangle}{\epsilon_a + \Omega - \epsilon_p}$$

$$\rho_{bwd}(a) = \sum_p \frac{\langle a | d_\Omega | p \rangle \langle p | \dots}{\epsilon_a - \Omega - \epsilon_p}$$

[Mårtensson-Pendrill J. Phys. France 46, 1949 (1985); Dahlström et al. Phys. Rev. A 86, 061402 (2012)]

RPAE-type effects in XUV-IR processes: (RPAE=Random Phase Approximation with Exchange)

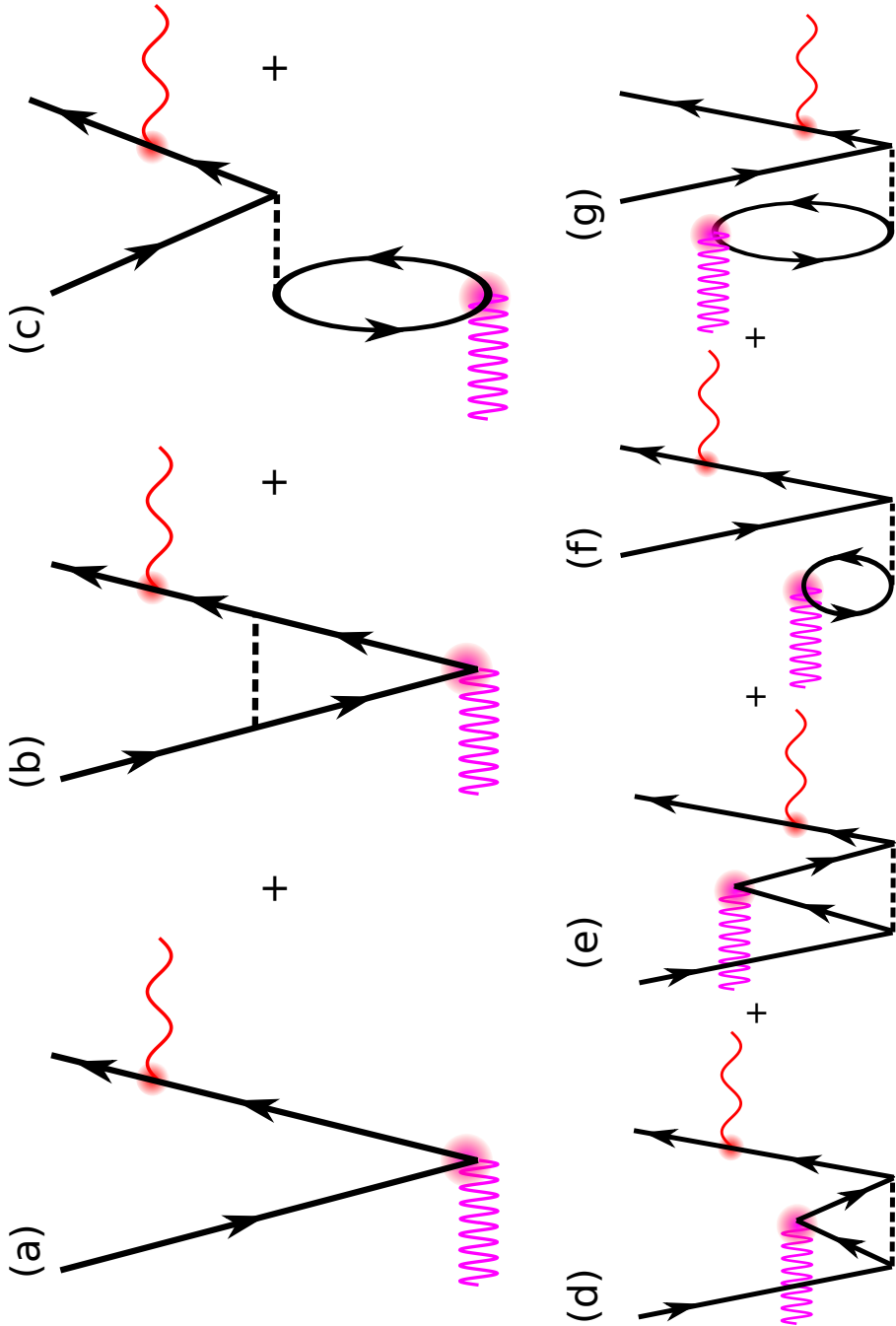
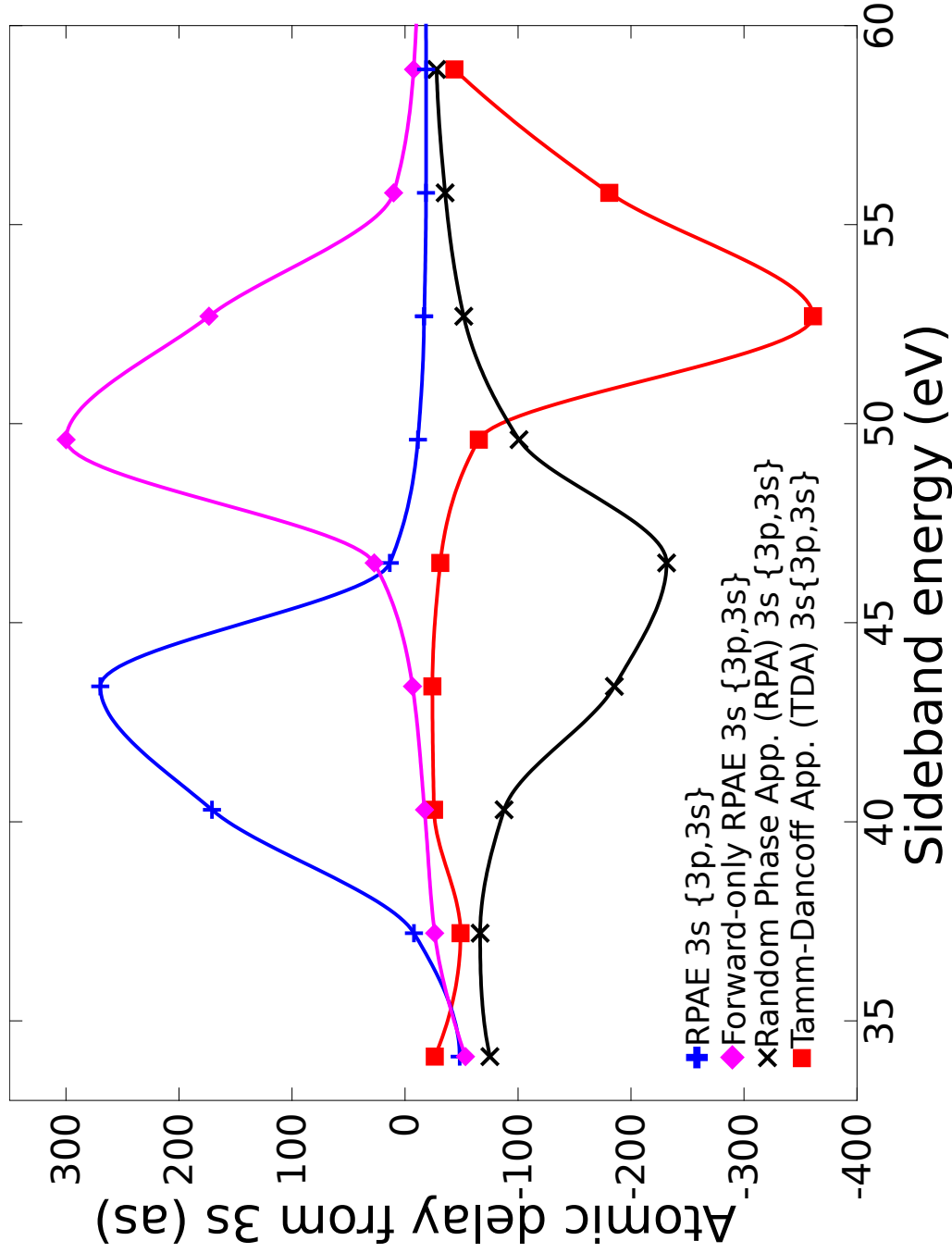


Figure: XUV photon absorbed first including RPAE-type correlation, and then interaction with the IR field last: (a) “Hartree-Fock”; (b) Direct; (c) Exchange; and (d)-(g) Ground-state correlations. Final-state correlation is not included.

“Worst case”: Correlation effects in $\text{Ar}3s^{-1}$
RABBITT delay depends strongly on correlation effects:

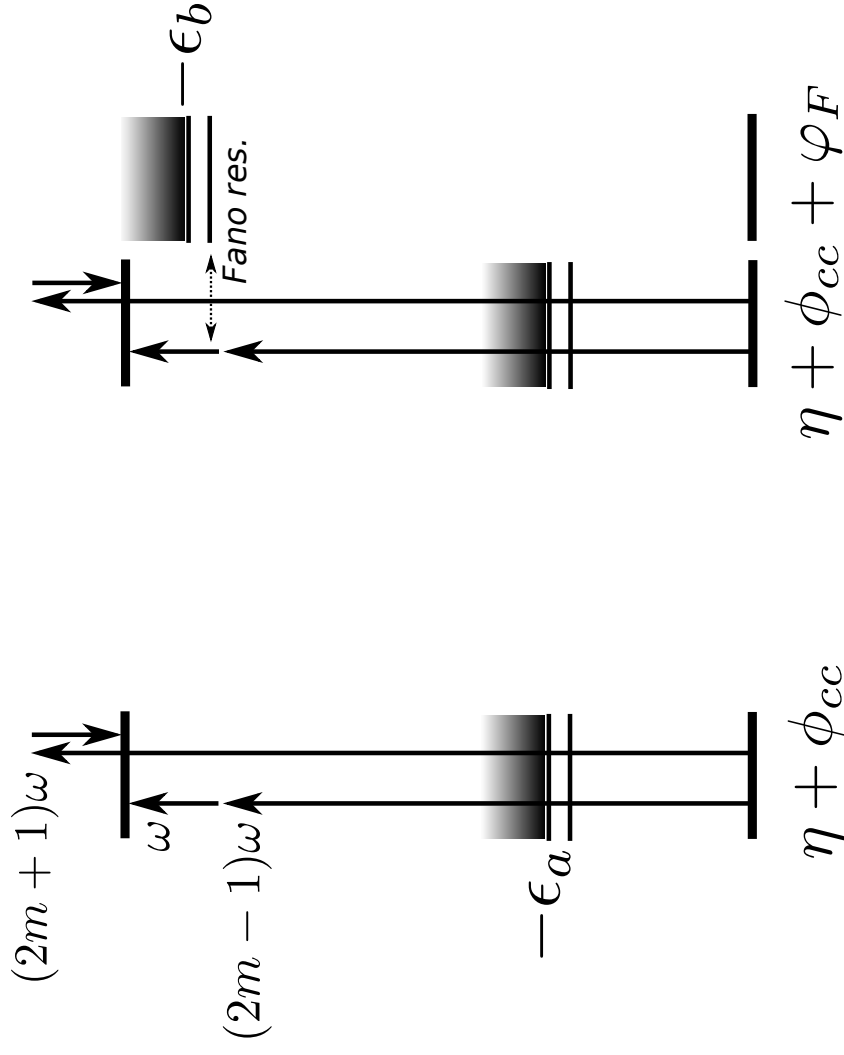


[Dahlström & Lindroth J.Phys.B 47 (2014) 124012]

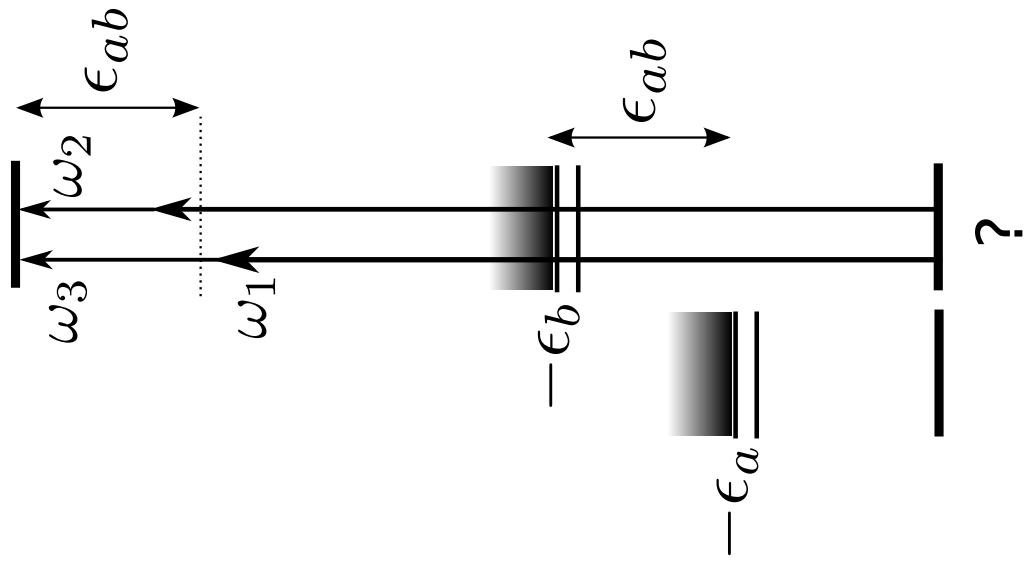
Overview of interferometric schemes

IR-driven electron dynamics \rightarrow XUV-stimulated hole transition

XUV HARMONICS + IR PROBE:

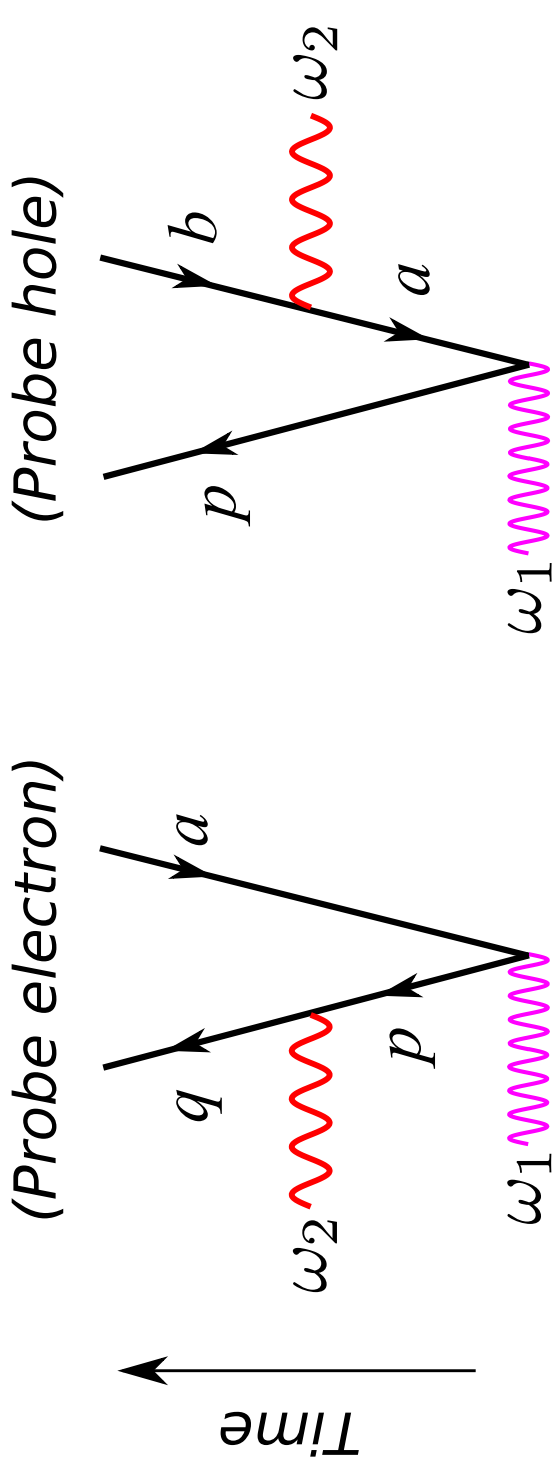


XUV PUMP AND XUV HARMONIC PROBE:



Considerations for a real probe scheme

Probe photoelectron or remaining hole in target?

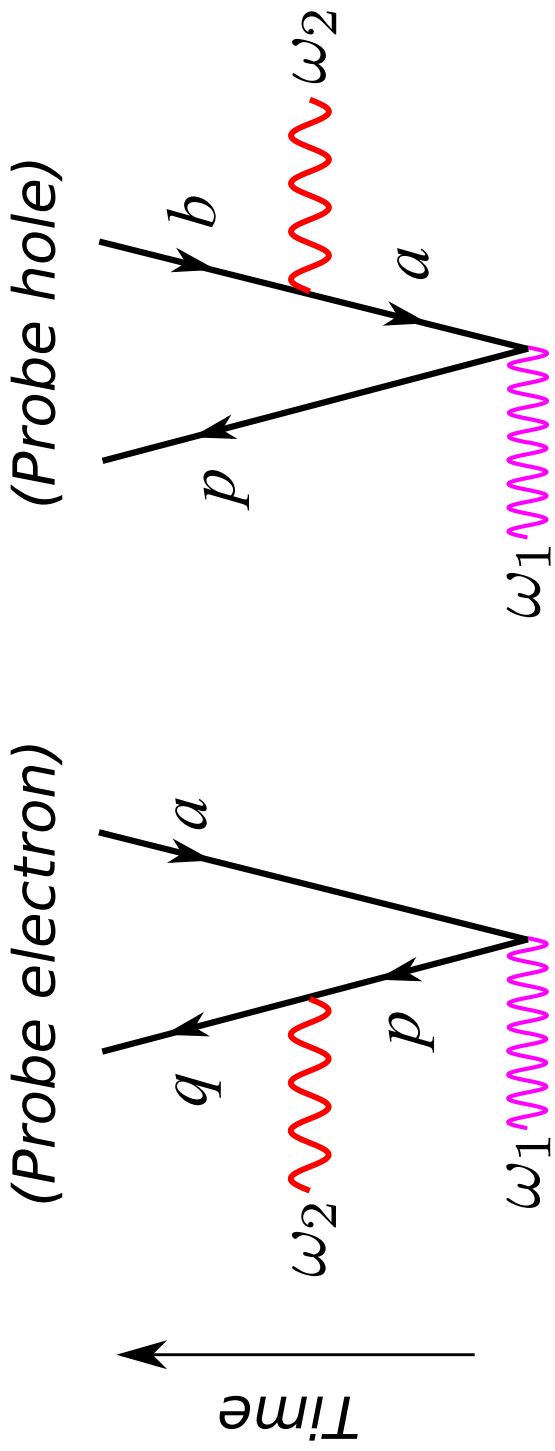


$$M_{qa}^{(e)}(\omega_1, \omega_2) = \lim_{\varepsilon \rightarrow 0^+} \frac{\int_n \langle q | O_2 | p \rangle \langle p | O_1 | a \rangle}{(\epsilon_a + \omega_1 - \epsilon_p + i\varepsilon)} \in \mathbb{C}$$

X

Considerations for a real probe scheme

Probe photoelectron or remaining hole in target?

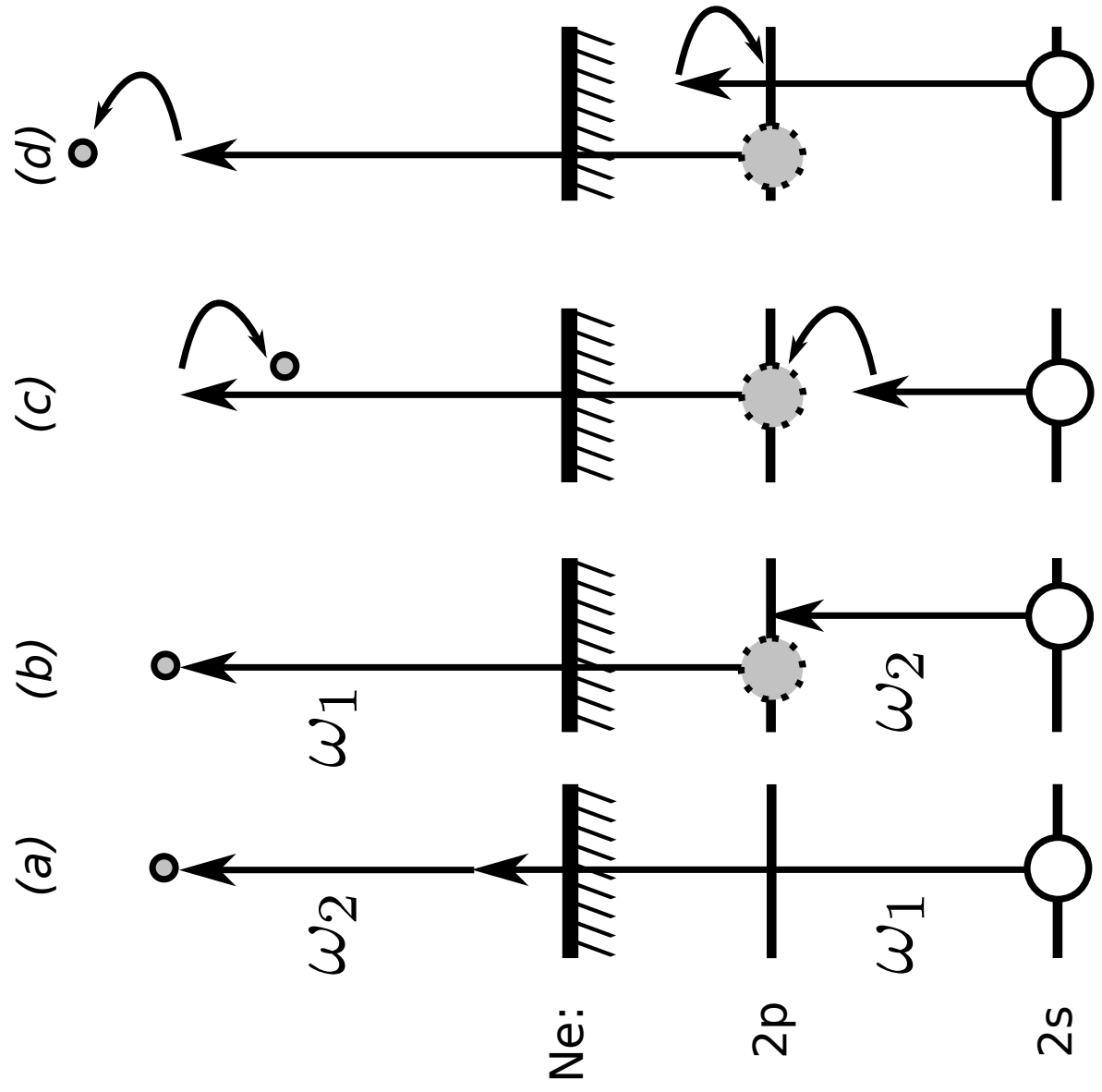


$$M_{qb}^{(e)}(\omega_1, \omega_2) = \lim_{\varepsilon \rightarrow 0^+} \frac{\int_n \langle q | O_2 | p \rangle \langle p | O_1 | a \rangle}{(\epsilon_a + \omega_1 - \epsilon_p + i\varepsilon)} \in \mathbb{C}$$
X

$$M_{pb}^{(h)}(\omega_1, \omega_2) = \frac{\langle a | O_2 | b \rangle \langle p | O_1 | a \rangle}{\underbrace{(\epsilon_a - \epsilon_b - \omega_2)}_{-\delta\omega}} \in \mathbb{R},$$
✓

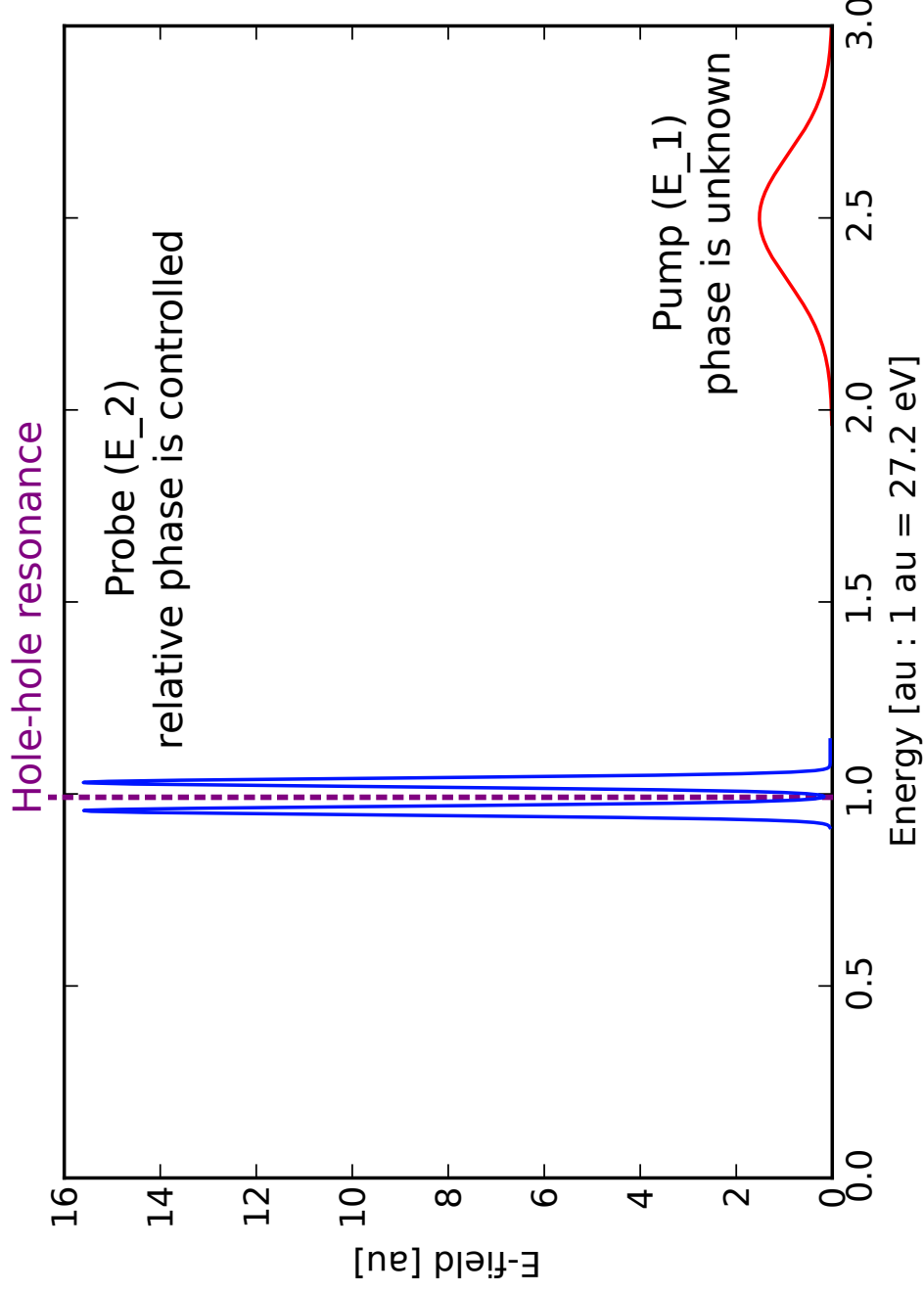
Cartoon of energy-shearing mechanism

Spectral shear of photoelectron due to energy sharing with hole



Setup of XUV fields

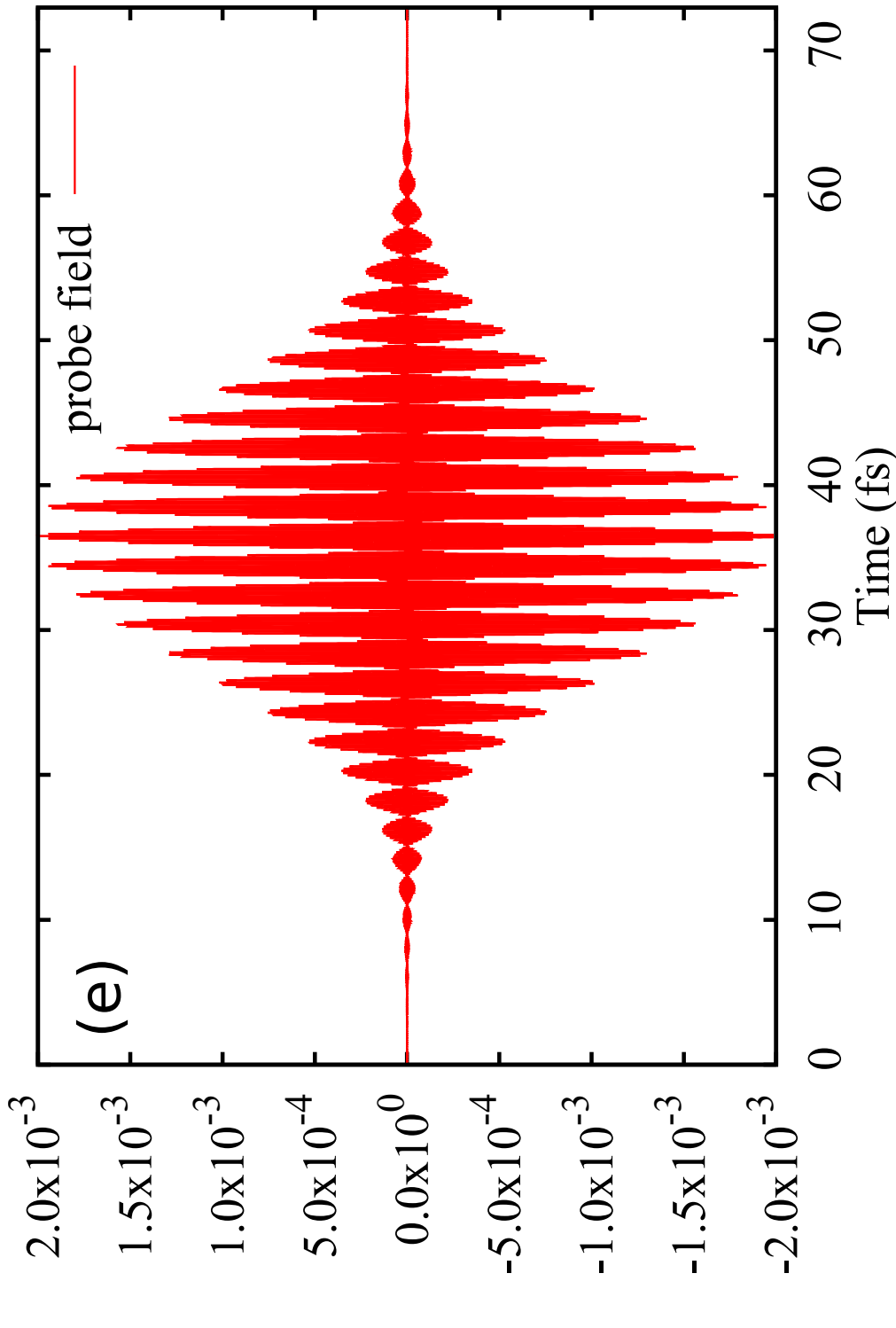
XUV field is divided in two parts as pump: E_1 and probe: E_2



- The pump E_1 : broad bandwidth with unknown phase, $\phi(\omega)$.
- The probe E_2 : has two components: above and below resonance [$\text{Ne}2p^{-1} \leftrightarrow \text{Ne}2s^{-1}$] with relative phase, φ .

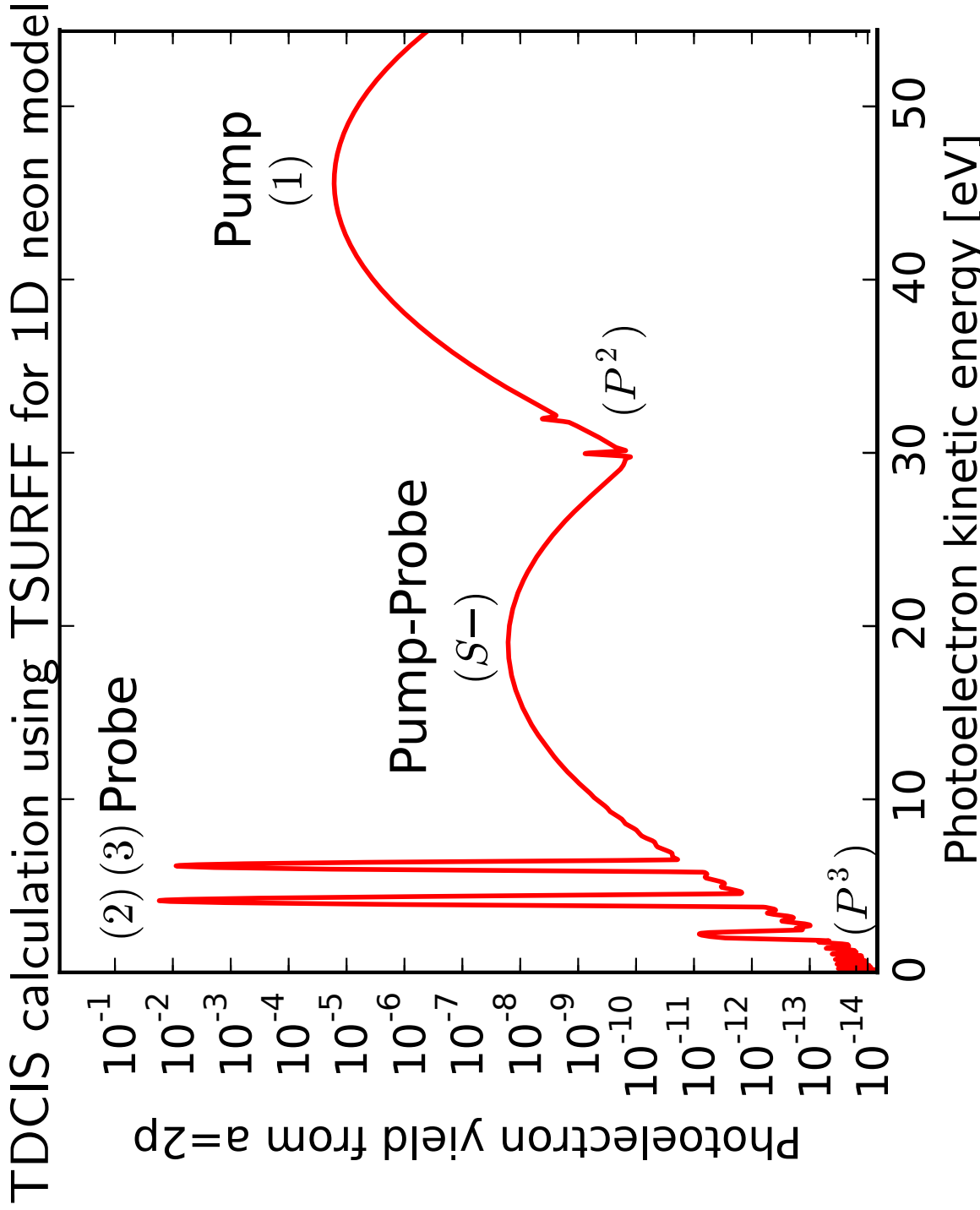
XUV probe field in the time-domain

Envelope-modulation on the attosecond timescale.



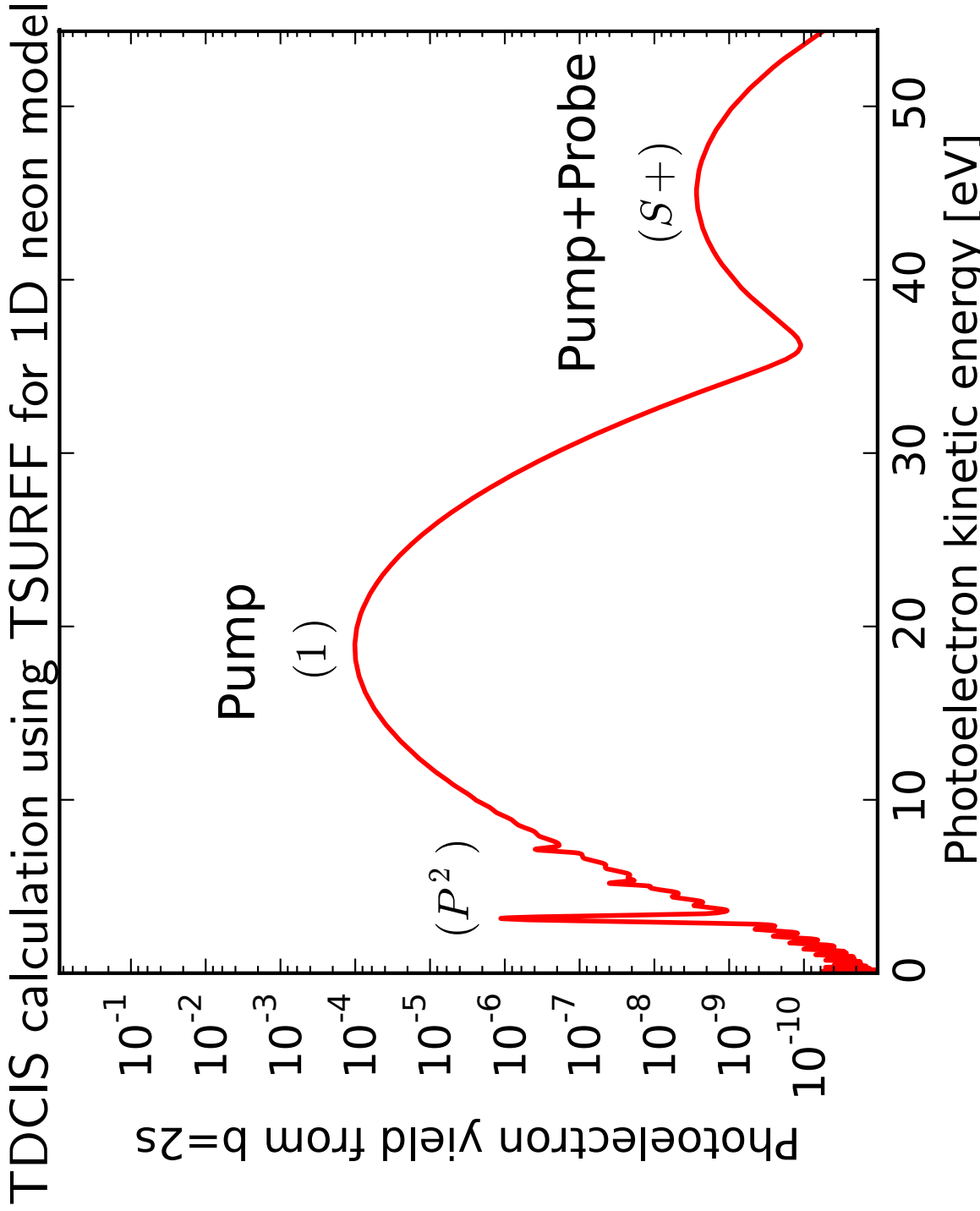
$$E_2(t) + E_3(t) \sim \cos[\delta\omega t - \frac{1}{2}(\phi_3 - \phi_2)] \cos[\omega_{ab}t - \frac{1}{2}(\phi_3 + \phi_2)]$$

Photoionization from outer orbital Time-Dependent Configuration-Interaction Singles



[Calculation by Jhih-An You in the group of Nina Rohringer]

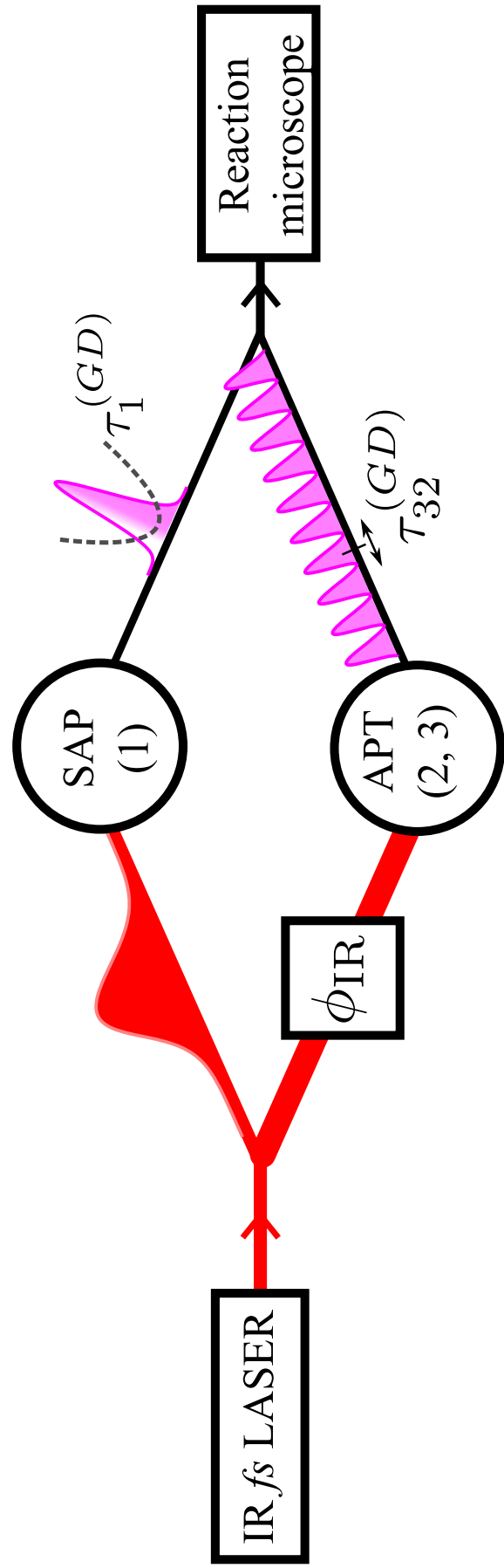
Photoionization from inner orbital Time-Dependent Configuration-Interaction Singles



[Calculation by Jhih-An You in the group of Nina Rohringer]

Overview of proposal

Coherent control of XUV pump and probe fields

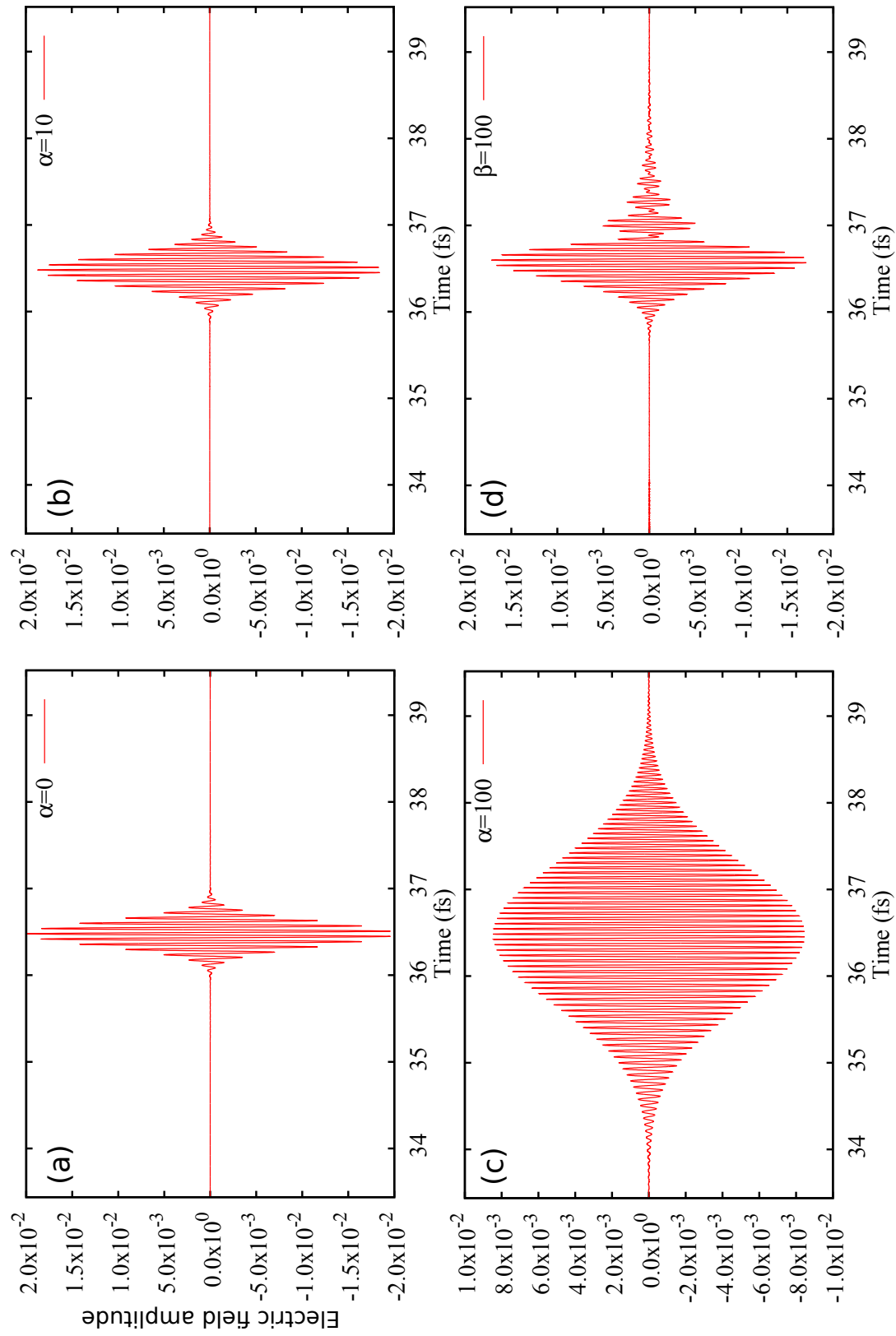


Isolated attosecond pulse and XUV probe fields are generated by high-order harmonic generation (HHG).

IR phase, ϕ_{IR} , is used to control XUV probe field.

Isolated attosecond pulses in the time-domain

The spectral phase changes the temporal structure of the pulses.

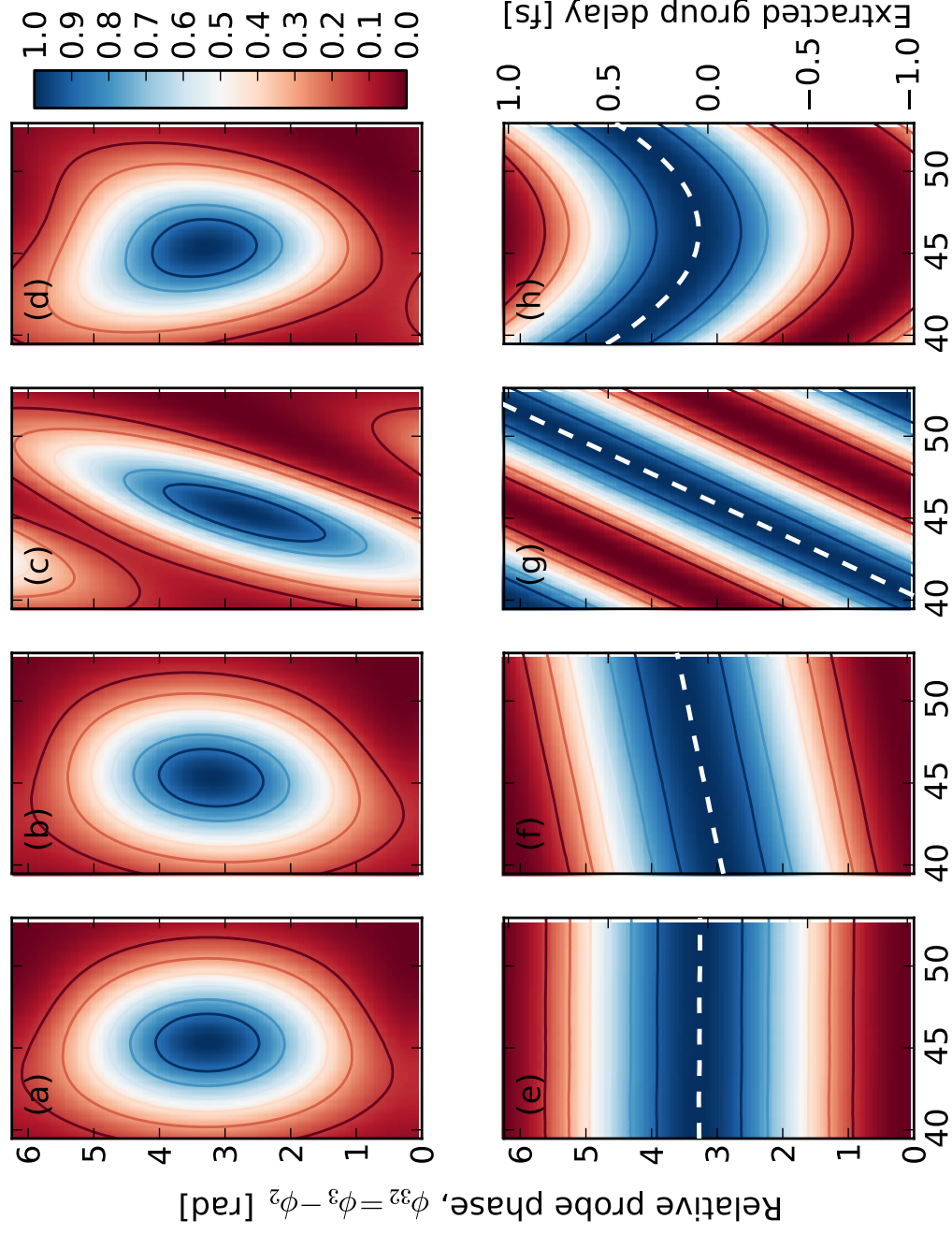


$$\arg[E_1(\omega)] = \phi_1(\omega) = \alpha(\omega - \omega_1)^2 + \beta(\omega - \omega_1)^3$$

Photoionization from inner orbital: ($S+$) peak

Time-Dependent Configuration-Interaction Singles

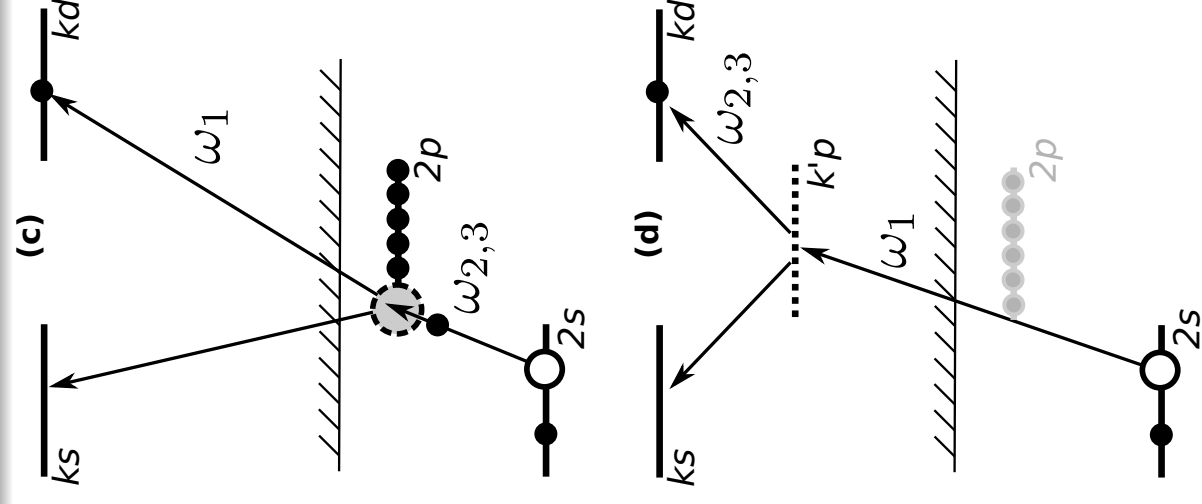
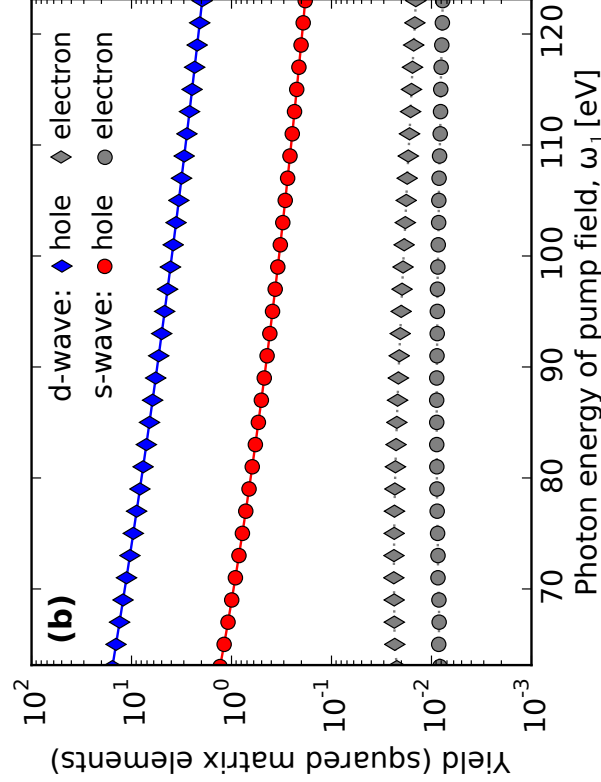
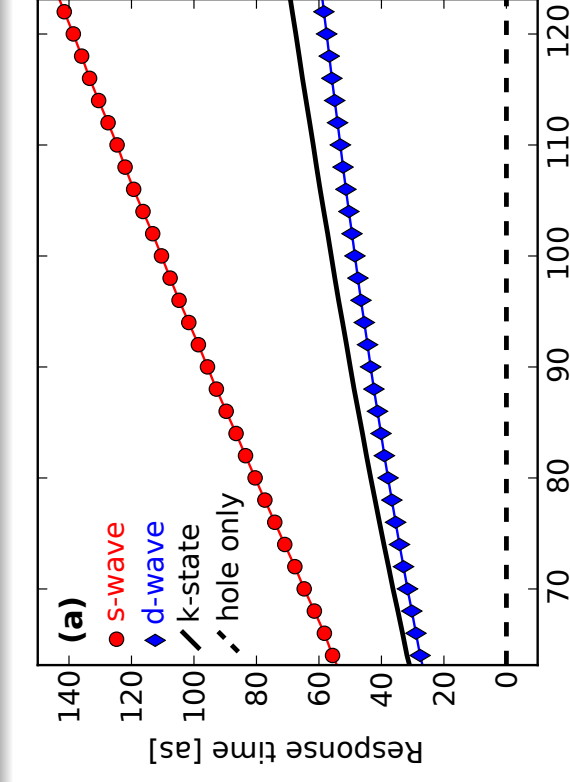
TDCIS calculation using TSURFF for 1D neon model



Kinetic energy of electron from inner state ($b=2s$) [eV]

Results for independent-particle model of neon (3D)

Response times and yields.



$$W_\gamma(\mathbf{k}) = |A_\gamma| - |B_\gamma| \cos[2\delta\omega(\tau_1^{(\text{GD})} - \tau_{3,2}^{(\text{GD})} - \tau_\gamma(\mathbf{k}))]$$

The complex amplitude for a transition from α to γ by first absorption of a photon from the pump field, $E_1(\omega_1)$, and then a photon from either probe field, E_f where $f = [2, 3]$, is

$$S_\gamma \approx \frac{1}{2\pi i} \sum_{f=2}^3 E_f E_1(\omega_{pc} - \omega_f) M_{pc}(\omega_{pc} - \omega_f, \omega_f), \quad (1)$$

where the two-photon matrix element contains two terms,

$$\begin{aligned} M_{pc}(\omega_1, \omega_f) &= M_{pc}^{(h)}(\omega_1, \omega_f) + M_{pc}^{(e)}(\omega_1, \omega_f) \\ &= \left[\sum_{b'} \frac{Zb'cZpb'}{\omega_f - \omega b'c} - \lim_{\xi \rightarrow 0^+} \sum_{p'} \frac{Zpp'Zp'c}{\omega_f - \omega pp' - i\xi} \right], \end{aligned} \quad (2)$$

corresponding to stimulated hole (h) and electron dynamics (e), respectively. Total energy conservation requires that $\omega_1 + \omega_f = \epsilon_p - \epsilon_c$. In writing Eq. (2) we have used second quantization to approximate the N -body matrix elements by single-particle transitions,

$$Z_{\beta'\alpha} \approx Z_{p'b'}, \quad Z_{\gamma\beta'} \approx -Z_{b'c}\delta_{p,p'} + Z_{pp'}\delta_{c,b'}.$$

Conclusion and Outlook

- Attosecond metrology using electron-laser interactions suffers from phase-lag and measurement-induced delays.
- Accurate calculation of these atomic delays is a big challenge [watch out for “TDLDA” (=linear response of LB94)*].
- New idea: Photoelectron shearing using stimulation of detuned hole-transition.
- The response time arises from the ratio of stimulated electron and hole dynamics by XUV fields.

Acknowledgment:

Eva Lindroth, Jhih-An You and Nina Rohringer.

* [M. Magrakvelidze, M. E. Madjet, G. Dixit, M. Ivanov, Himadri S. Chakraborty: arXiv:1505.01058]

Thank you for your attention!

